



A tri-stable structure of piezoelectric-electromagnetic composite energy harvester (TPEEH)

Zhaoyang Peng¹ · Fang Song¹ · Yuzhong Xiong²

Received: 31 July 2021 / Accepted: 10 January 2023 / Published online: 31 January 2023
© The Author(s), under exclusive licence to Springer-Verlag GmbH Germany, part of Springer Nature 2023

Abstract

In order to improve the energy conversion performance and efficiency of the bi-stable piezoelectric-electromagnetic composite energy collector, based on the typical piezoelectric- electromagnetic composite energy collector, a tri-stable piezoelectric-electromagnetic composite energy collector with electromagnetic power generation device was developed and designed. The mathematical model of TPEEH is analyzed and the formula of its potential energy function is derived. The effects of frequency and load resistance on voltage and power are studied. The results show that when the magnetic distance is $d = 16$ mm and the external excitation frequency is 10.2 Hz, the maximum output voltage of the TPEEH system is 12.0539 V, and the maximum output power is 278.39 μ W when the external load is 600 k Ω . Experimental results show that the designed TPEEH has higher output voltage and higher output power than the traditional TPEEH. Therefore, TPEEH has lower frequency, wider frequency band, higher output voltage and power, improving energy conversion performance and efficiency.

1 Introduction

The rapid development of human society is inseparable from the support of energy, and the development of traditional fossil energy will cause damage to the environment to a certain extent. produce a certain degree. As a result, with the gradual depletion of traditional energy sources and the continuous deterioration of the natural environment of society, the development and utilization of new energy sources have attracted more and more attention from all over the world. Vibration energy is widely distributed in the natural environment since vehicles, factories, subways, and human movements will all produce vibrations, and will not be affected by the weather (Xia et al. 2015; Arroyo

et al. 2012). Therefore, harvesting this kind of renewable and clean energy which has characteristics of abundant reserves and easy collection to replace traditional fossil fuels is important (Khaligh et al. 2009).

Currently, there are three common energy harvesting techniques (Wang et al. 2021; Mikio et al. 1996): first, electromagnetic energy harvesting; second, piezoelectric energy harvesting; and third, electrostatic energy harvesting. In terms of collecting vibration energy, scholars have mainly used piezoelectric energy harvesting for harvesting vibration energy in the environment. The current piezoelectric energy harvesters are mainly available in basic structures such as spiral, S-shaped and cantilever beam type (Shindo et al. 2014; Ali et al. 2014; Liu et al. 2014; Yuzhong et al. 2020). Due to the simple structure and strong operability of the cantilever beam design, the main structures proposed and already manufactured by researchers are: piezoelectric single-chip structure (Johnson et al. 2006), piezoelectric double-chip structure (Sodano et al. 2004) and piezoelectric double-chip structure with a mass block at the end of the cantilever beam (Jiang et al. 2005). However, a single piezoelectric energy harvesting approach cannot match the large amount of environmental vibration energy with different frequency components in nature (Roundy et al. 2003), and some piezoelectric energy harvesters require additional initial

✉ Fang Song
songfang2005@163.com

Zhaoyang Peng
814799563@qq.com

Yuzhong Xiong
362996309@qq.com

¹ School of Mechanical and Automotive Engineering, Shanghai University of Engineering Science, 333 Longteng Road, Songjiang District, Shanghai 201620, China

² Shanghai Awinic Technology Co., Ltd, Shanghai 201100, China

voltage (Roundy et al. 2004). The results of the study show that piezoelectric energy harvesting has the advantage of large voltage output and high power density, and the electromagnetic energy harvesting has the advantage of large current output and low energy consumption. No matter how novel and unique the structure of the single-mechanism energy harvester is, there are more or less shortcomings, such as not being able to output large current and large voltage at the same time, limited output power and conversion efficiency, single output characteristics, and weak environmental adaptability.

In response to the above problems, scholars have proposed vibration energy harvesters with mixed-mode structures of different energy harvesting methods which may improve the efficiency of energy harvesting, such as integrating piezoelectricity and friction together to increase their charge density through charge injection and polarization (Wang et al. 2016; Yang et al. 2015); other related researchers have compounded piezoelectric and electromagnetic energy harvesters for extensive researches (Iqbal et al. 2018; Toyabur et al. 2018; Javed et al. 2019; Bolat et al. 2019; Yuzhong et al. 2022). However, there still exist flaws in these composite harvesters, such as poor system coupling, low conversion efficiency, poor environmental adaptability, etc.

Therefore, in this paper, a hybrid piezoelectric-electromagnetic energy harvesting device would be proposed. It is used to harvest more energy and reduce the loss of energy thus improving its harvesting efficiency. The results show that this hybrid energy harvester has a maximum system output voltage of 12.0539 V at a magnetic distance of 16 mm and an external excitation frequency of 10.2 Hz, and a maximum output power of 278.39 μW at an external load of 600 k Ω . This design can effectively harvest vibration energy for wireless sensing networks. The device can not only collect the vibration energy effectively, but also can be used by the sensor effectively.

2 Theoretical model of TPEEH

2.1 Structure and working principle

The structure of the hybrid piezoelectric-electromagnetic energy harvester designed in this paper is shown in Fig. 1.

The structure is mainly divided into two parts, the left side is the cantilever beam structure of piezoelectricity, and the right side is the EMG structure. In the piezoelectric structure, a cantilever beam structure is used to make a pair of piezoelectric sheets uniformly cover the upper and lower

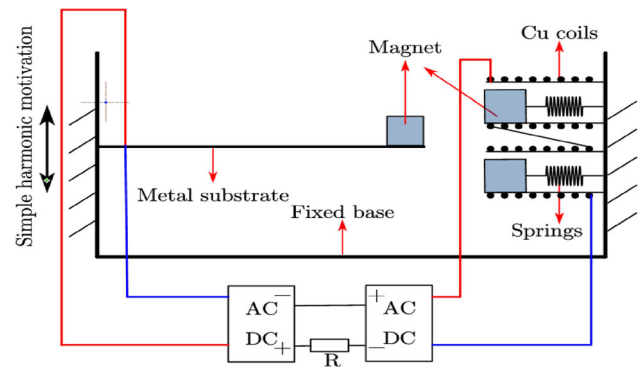


Fig. 1 Power generation structure of piezoelectric-electromagnetic composite collector

surfaces of the root of the cantilever beam, and a permanent magnet is fixedly connected to the end of the cantilever beam; in the EMG structure, one end of three identical permanent magnets is connected to the spring fixed to a cardboard, and three identical copper coils on the other end of the three wrap the permanent magnets in them.

When being stimulated by external factors, since the piezoelectric part on the left is connected to a fixed weight of the magnet, the cantilever beam will swing up and down which may deform the piezoelectric sheets fixed on the upper and lower sides of the cantilever beam, thus generating current and voltage through the external circuit. However, on the right side of the electromagnetic part, when being externally stimulated, the cantilever beam will swing up and down due to the weight of the magnet at the end, and the magnet fixed at the end also swings up and down with it, which will then affect the three permanent magnets fixed on the bracket. According to relevant principles of the magnet, magnetized by the magnet at the end of the cantilever beam, the external magnet fixed on the bracket would move backward to compress the spring, and at the same time, the magnetic inductance and magnetic flux of the external magnet in the copper coil will change. Also, according to Faraday's law of electromagnetic induction, the copper coil will generate an induced current due to the change of magnetic flux in the coil.

The unique feature of this structure is that it combines two different energy harvesting methods, complementing each other with their own strengths. In this way, the two collection methods can eliminate or reduce the limitations of one collection method, thus further improving its energy collection and conversion efficiency. The end magnet acts on the external magnet so that it cuts the magnetic induction lines, causing the magnetic flux in the copper coil to change, thus generating an induced current. According to Newton's third law, the external magnet generates a force

of the same magnitude but in the opposite direction to the end magnet of the cantilever beam which will oscillate up and down constantly due to the force of the right part of the external magnet, so that the above process will be repeated until the system between the magnets and the entire structure of the device reaches balance again. Compared to the traditional piezoelectric cantilever beam structure, the innovation lies in the collector’s long duration after receiving external excitation. Also, compared to some three-dimensional steady-state structure collectors, the addition of copper coils and springs has made the whole system combined into a composite energy collector, which would greatly improve collection efficiency and avoids the drawbacks of single energy collection modes.

2.2 Theoretical analysis

A beam of copper material is used in this experiment. The length is 90 mm, the total thickness of the cantilever beam is 0.618 mm, the high span ratio $H/L = 0.618/90 = 0.0069 \ll 0.2$, so the shear deformation could be

relatively high span of the cantilever beam. Ignoring the shear deformation, the displacement field is as follows:

The displacement in the x -direction is

$$s_1 = s_0 - s_x = s_0 - z \frac{\partial v_0}{\partial x} \tag{1a}$$

The displacement in the Z -direction is

$$s_3 = v_0 + W \sin \Omega t \tag{1b}$$

where: s_1 is the absolute displacement in X direction; s_3 is the absolute displacement in Z direction; s_0 is the relative displacement in X direction; v_0 is the relative displacement in Z direction.

According to Hamilton’s principle, the nonlinear dynamics equation of the piezoelectric-electromagnetic composite power generation structure is established as:

$$\sigma \int_{t_0}^{t_1} (T - U) dt + \int_{t_0}^{t_1} \sigma W_0 dt = 0 \tag{2}$$

The repulsive force of the magnet in the equilibrium position is:

$$F = \frac{3}{2(1+d)} \times \frac{bc}{2\mu_r} \times \frac{B_r^2}{\pi^2} \times \frac{d_g \mp v}{\sqrt{d^2 + (d_g \mp v)^2}} \times \left(\tan^{-1} \frac{bc}{2d\sqrt{b^2 + c^2 + 4d^2}} - \tan^{-1} \frac{bc}{2d(a+d)\sqrt{b^2 + c^2 + 4(a^2 + d^2)}} \right)^2 \tag{3}$$

ignored in the system. Therefore, Euler–Bernoulli beam theory would be adopted to study the piezoelectric cantilever beam structure.

Figure 2 shows the geometric model of the system. Only the transverse electric field is considered because of the

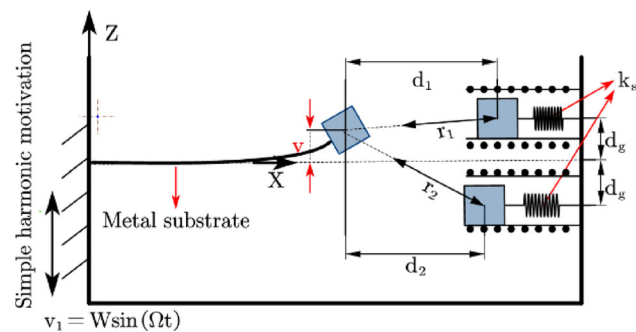


Fig. 2 Nonlinear magnetic model of the system magnet

where: a is the length of the magnet; b is the width of the magnet; c is the height of the magnet; d is the magnetic distance; μ_r is the vacuum permeability; B_r is the performance parameter of the magnet.

The repulsive force F between the magnets is decomposed as the change in the vertical displacement v of the magnets; the horizontal component force F_x varies with the change in the horizontal displacement x of the magnets, and its magnitude is:

$$F_z = F \times \frac{d_g \mp v}{\sqrt{d^2 + (d_g \mp v)^2}} \tag{4}$$

Substituting Eq. (3) into Eq. (4) could get:

$$F_z = \frac{3}{2(1+d)} \times \frac{bc}{2\mu_r} \times \frac{B_r^2}{\pi^2} \times \frac{d_g \mp v}{\sqrt{d^2 + (d_g \mp v)^2}} \times \left(\tan^{-1} \frac{bc}{2d\sqrt{b^2 + c^2 + 4d^2}} - \tan^{-1} \frac{bc}{2d(a+d)\sqrt{b^2 + c^2 + 4(a^2 + d^2)}} \right)^2 \times \frac{d_g \mp v}{\sqrt{d^2 + (d_g \mp v)^2}} \tag{5}$$

Make

The total potential energy of the system is:

$$k_1 = \frac{3}{2(1+d_1)} \times \frac{bc}{2\mu_r} \times \frac{B_r^2}{\pi^2} \times \frac{d_g - v}{\sqrt{d_1^2 + (d_g - v)^2}} \times \left(\tan^{-1} \frac{bc}{2d_1\sqrt{b^2 + c^2 + 4d_1^2}} - \tan^{-1} \frac{bc}{2d_1(a+d_1)\sqrt{b^2 + c^2 + 4(a^2 + d_1^2)}} \right)^2 \tag{6}$$

$$k_2 = \frac{3}{2(1+d_2)} \times \frac{bc}{2\mu_r} \times \frac{B_r^2}{\pi^2} \times \frac{d_g + v}{\sqrt{d_2^2 + (d_g + v)^2}} \times \left(\tan^{-1} \frac{bc}{2d_2\sqrt{b^2 + c^2 + 4d_2^2}} - \tan^{-1} \frac{bc}{2d_2(a+d_2)\sqrt{b^2 + c^2 + 4(a^2 + d_2^2)}} \right)^2 \tag{7}$$

$$U = \frac{1}{2} \int_y \left[C \left(\frac{\partial s_0}{\partial x} + \frac{1}{2} \left(\frac{\partial w_0}{\partial x} \right)^2 - z \left(\frac{\partial^2 w_0}{\partial x^2} \right)^2 + \frac{Vd}{h_3 - h_4} \left(\frac{\partial s_0}{\partial x} + \frac{1}{2} \left(\frac{\partial w_0}{\partial x} \right)^{\frac{\partial w_0}{\partial x}} - z \left(\frac{\partial^2 w_0}{\partial x^2} \right) \right) \right] dy - \frac{1}{2} \int_y \left[-\frac{Vd}{h_3 - h_4} \left(\frac{\partial s_0}{\partial x} + \frac{1}{2} \left(\frac{\partial w_0}{\partial x} \right) \frac{\partial w_0}{\partial x} - z \left(\frac{\partial^2 w_0}{\partial x^2} \right) \right) + \frac{\varepsilon V^2}{(h_3 - h_4)^2} \right] dy + \left(\frac{k_2 d_g}{(d_2^2 + d_g^2)^{1/2}} - \frac{k_1 d_g}{(d_2^2 + d_g^2)^{1/2}} \right) v_0 + \frac{1}{2} \left(\frac{k_2 d_2^2}{(d_2^2 + d_g^2)^{3/2}} - \frac{k_1 d_1^2}{(d_1^2 + d_g^2)^{3/2}} \right) v_0^2 + \frac{1}{6} \left(\frac{-3k_2 d_2^2 d_g}{(d_2^2 + d_g^2)^{5/2}} + \frac{3k_1 d_1^2 d_g}{(d_1^2 + d_g^2)^{5/2}} \right) v_0^3 + \frac{1}{24} \left(\frac{-3k_2 d_2^4 + 12k_2 d_2^2 d_g^2}{(d_2^2 + d_g^2)^{7/2}} + \frac{-3k_1 d_1^4 + 12k_1 d_1^2 d_g^2}{(d_1^2 + d_g^2)^{7/2}} \right) v_0^4 + \frac{1}{120} \left(\frac{45k_2 d_2^4 d_g - 60k_2 d_2^2 d_g^3}{(d_2^2 + d_g^2)^{9/2}} + \frac{-45k_1 d_1^4 d_g + 60k_1 d_1^2 d_g^3}{(d_1^2 + d_g^2)^{9/2}} \right) v_0^5 + \frac{1}{720} \left(\frac{45k_2 d_2^6 - 540k_2 d_2^4 d_g^2 + 360k_2 d_2^2 d_g^4}{(d_2^2 + d_g^2)^{11/2}} + \frac{45k_1 d_1^6 - 540k_1 d_1^4 d_g^2 + 360k_1 d_1^2 d_g^4}{(d_1^2 + d_g^2)^{11/2}} \right) v_0^6 + \frac{k_1^2 d_1^2}{2k_s [d_1^2 + (d_g - v_0)^2]} + \frac{k_2^2 d_2^2}{2k_s [d_2^2 + (d_g + v_0)^2]} \tag{8}$$

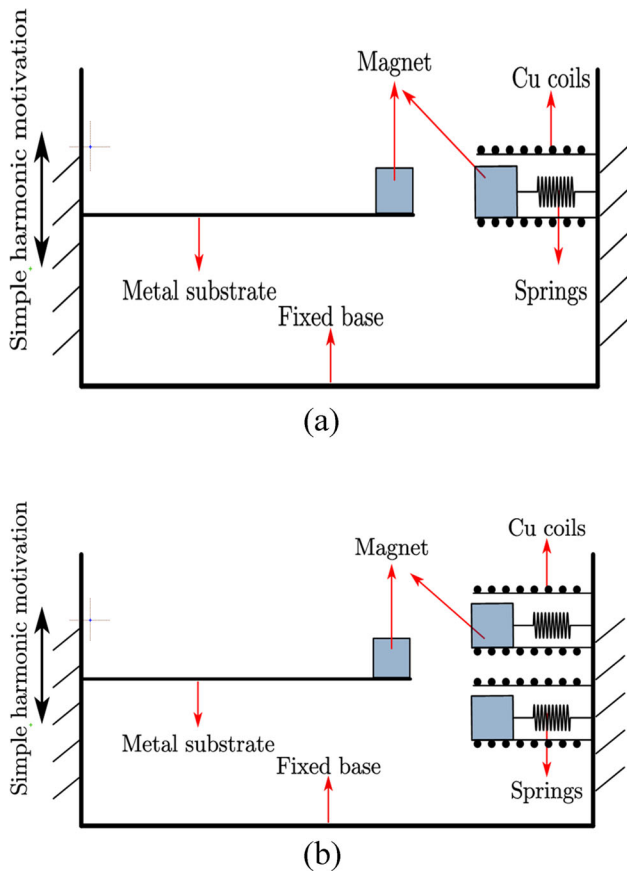


Fig. 3 Piezoelectric-electromagnetic composite energizer power generation structure. **a** The bi-stable and **b** the tri-stable

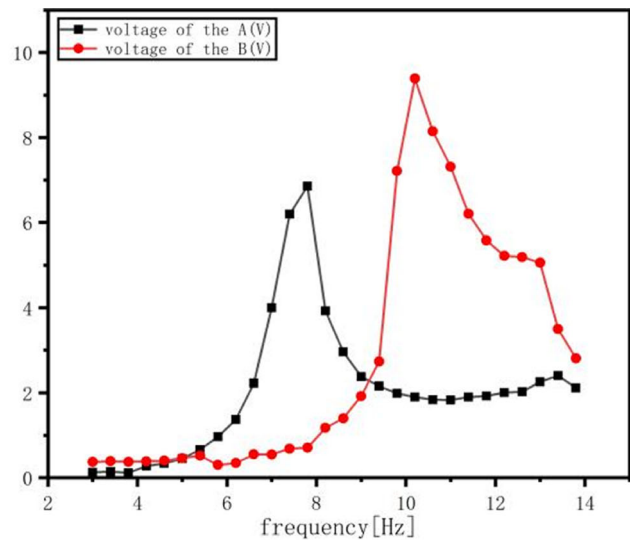
Make the equation of the total potential energy discrete in the first order.

Make

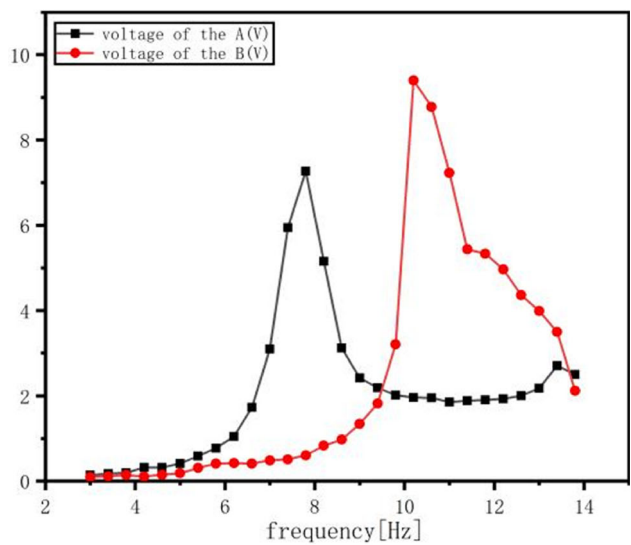
$$v_0 = \phi(x)v_1(t) \tag{9}$$

Substituting Eq. (9) into Eq. (8) and multiplying both sides of the equation by $\phi_j(x)$, and integrating over the interval [0,1] could get:

$$\begin{aligned}
 U = & I_{11}v_1^6 + I_{22}v_1^5 + I_{33}v_1^4 + I_{44}v_1^3 + I_{55}v_1^2 + I_{66}v_1 + I_{21} \\
 & \times \left(\frac{I_{12}}{I_{12} + I_{14} - 2I_{15}v_1 + v_1^2} \right) + I_{22} \\
 & \times \left(\frac{I_{13}}{I_{13} + I_{14} + 2I_{15}v_1 + v_1^2} \right) - I_{23}
 \end{aligned} \tag{10}$$



(a)



(b)

Fig. 4 The frequency-voltage relation curve of structure A and structure B in different magnetic distances. **a** The magnetic distance is 14 mm and **b** the magnetic distance is 15 mm

3 Experiments and results

3.1 Comparative study of the power generation characteristics of the bi-stable and the ti-stable

In this experiment, the conventional bi-stable piezoelectric-electromagnetic generation structure (hereinafter referred to as the structure A) and the tri-stable piezoelectric-electromagnetic generation structure (hereinafter referred to as the structure B) were compared. Also, the effects of external excitation frequency and magnetic distance on the

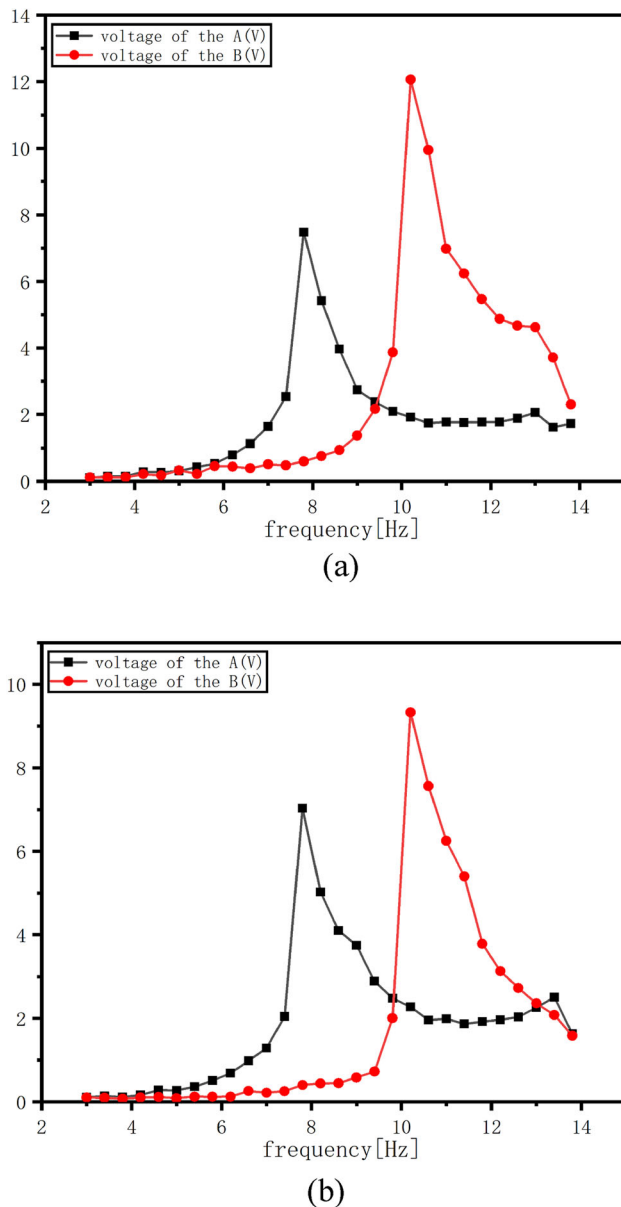


Fig. 5 The frequency-voltage relation curve of structure A and structure B in different magnetic distances. **a** The magnetic distance is 16 mm and **b** the magnetic distance is 17 mm

generation characteristics of both structures were analyzed to get some experimental regular features.

Based on the traditional bi-stable piezoelectric-EM power generation structure, a tri-stable piezoelectric-EM power generation structure with the introduction of springs and coils would be further proposed. Both the bi-stable composite structure and the tri-stable composite structure are based on the electromechanical coupling of piezoelectricity and electromagnetism, the two structures were combined through appropriate harvesting circuits to effectively improve the energy harvesting efficiency of the system. The bi-stable piezoelectric-EM generation

structure and the tri-stable piezoelectric-EM generation structure are shown in Fig. 3.

The power generation characteristics of bi-stable and tri-stable structures are the focus of this experiment. Both structures are subjected to the same simple harmonic excitation, and the piezoelectric cantilever beam is forced to vibrate, thus driving the end magnet and the external magnet to vibrate. The external excitation amplitude is set to 2.5 V, the external excitation frequency is 3–13.8 Hz, and the step size is 0.4 Hz. When the magnetic distance is less than 14 mm, which is too small, the magnetic force is too large, the piezoelectric cantilever beam vibrates at a small amplitude, and the oscilloscope shows that the output voltage is very small; when the magnetic distance is greater than 18 mm, which is too large, the magnetic force decreases, and the steady state of the system disappears, which has no research significance. As a result, the magnetic distance is set to 14 mm, 15 mm, 16 mm, 17 mm, and 18 mm in the experiment. There are five groups of experiments in total, in which the output performance of the bi-stable and the tri-stable is compared by controlling variables. In this experiment, the efficiency of the power generation is the coupling output voltage of the system being divided by the laying volume of the beam. Also, the piezoelectric material is fully laid in both upper and lower layers, and the laying volume of the piezoelectric material is $90 \text{ mm} \times 20 \text{ mm} \times 0.03 \text{ mm} = 54 \text{ mm}^3$.

In the first set of experiments, the magnetic distance was set to 14 mm for both bi-stable and tri-stable states. The experimental data are shown in Fig. 4a. Data show that the maximum output voltage of the bi-stable structure is 6.8566 V and the generation efficiency is 0.127 V/mm³.

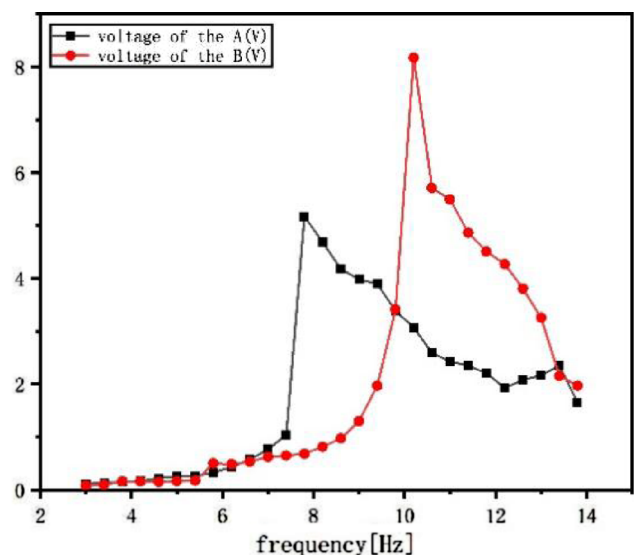
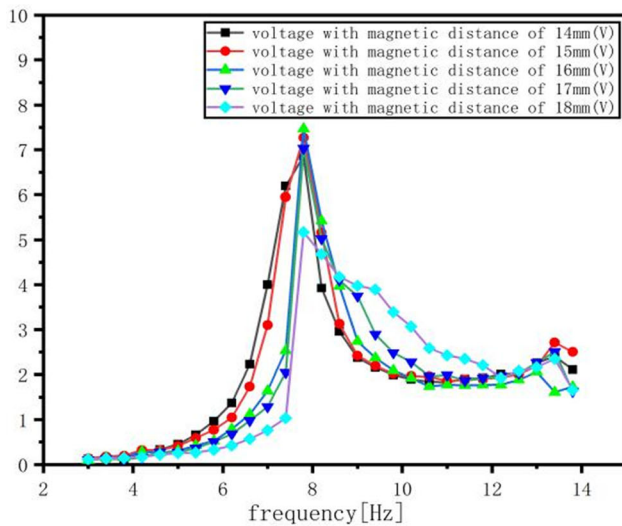
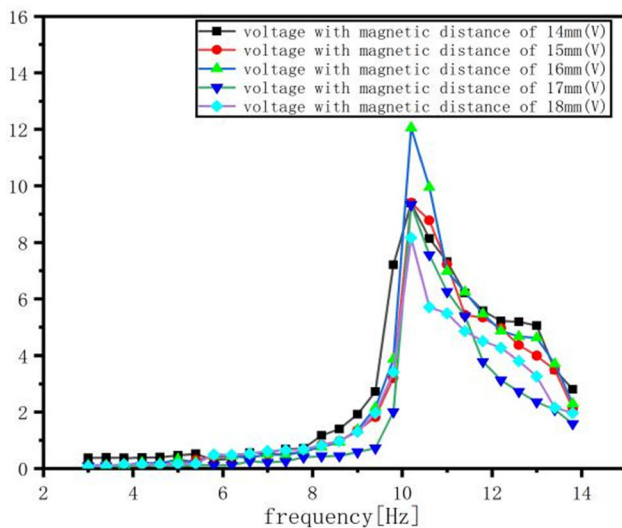


Fig. 6 The frequency-voltage relation curve of structure A and structure B when the magnetic distance is 18 mm



(a)



(b)

Fig. 7 The frequency-voltage relation curve of the system with different initial magnetic distance. **a** The structure A and **b** the structure B

The maximum output voltage of the tri-stable structure is 9.385 V and the generation efficiency is 0.174 V/mm³. Results show that the output voltage of the tri-stable structure is higher than that of the bi-stable structure and the generation efficiency is improved. The output of the bi-stable structure reaches the maximum at 7.8 Hz, while the output of the tri-stable structure reaches the maximum at 10.2 Hz, which means that the bi-stable structure responds faster than the tri-stable one. What’s more, the output voltage of the bi-stable structure is higher than that of the tri-stable structure when the frequency is low. But as the frequency increases, the output of the bi-stable structure decreases and the output of the tri-

stable structure increases. From the above results, a preliminary judgment could be obtained that the tri-stable structure is more efficient and has the largest output voltage; however, the output voltage of the bi-stable structure is higher than that of the tri-stable structure at lower frequencies.

In the second group of experiments, the magnetic distance was set to 15 mm for both bi-stable and tri-stable structures. The experimental data are shown in Fig. 4b which shows that the output voltage of the tri-stable structure is higher than that of the bi-stable structure, and the power generation efficiency is improved.

In the third group of experiments, the magnetic distance of both bi-stable and tri-stable structures was set to 16 mm. The experimental data are shown in Fig. 5a, from which some important findings could be get that the maximum output voltage of the bi-stable is 7.4717 V, and the generation efficiency is 0.138 V/mm³. The maximum output voltage of the tri-stable is 12.0539 V, and the generation efficiency is 0.223 V/mm³. Results show that the output voltage of the tri-stable is higher than that of the bi-stable, and its generation efficiency is relatively higher. When the external excitation frequency is higher, the output voltage of the tri-stable is significantly higher than that of the bi-stable. The experimental data in this step would further verify that the tri-stable structure has better power generation characteristics than the bi-stable structure.

In the fourth group of experiments, the magnetic distance of both bi-stable and tri-stable was set to 17 mm. The experimental data are shown in Fig. 5b which shows that the maximum output voltage of the bi-stable is 7.0314 V, and the generation efficiency is 0.130 V/mm³. However, the maximum output voltage of the tri-stable is 9.3298 V, and the generation efficiency is 0.173 V/mm³. The above

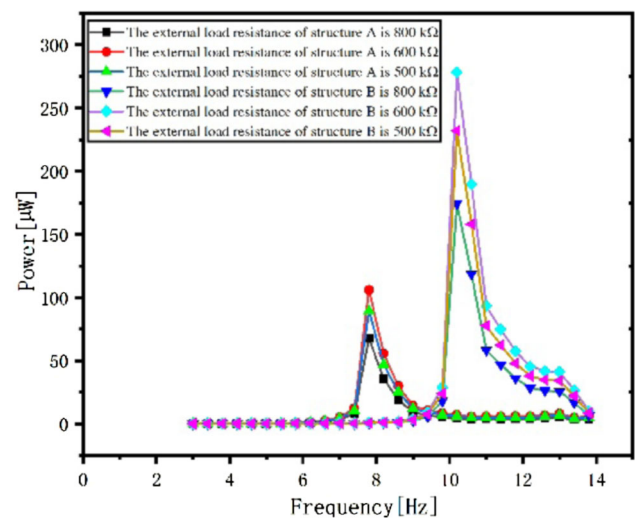


Fig. 8 Frequency versus power curve for different external loads

experimental data show that the output voltage of tri-stable is higher than that of the bi-stable, and its generation efficiency is greatly improved. From the above four groups of experiments, a preliminary judgment could be obtained that the output voltage of bi-stable is higher than that of the tri-stable at a lower external excitation frequency. As the frequency increases, the output voltage of bi-stable decreases and that of the tri-stable increases. However, the maximum output voltage of the bi-stable is always less than that of the tri-stable, and the generation efficiency of the tri-stable is higher than that of the bi-stable.

In the fifth group of experiments, the magnetic distance was set to 18 mm for both bi-stable and tri-stable structures. The experimental data are shown in Fig. 6, from which it can be concluded that the maximum output voltage of bi-stable is 5.171 V, and its generation efficiency is 0.096 V/mm³. The maximum output voltage of the tri-stable is 8.1709 V, and its generation efficiency is 0.151/mm³. The maximum output voltage of bi-stable is obviously lower than that of the tri-stable.

The voltage-frequency relationship between the structure A and structure B is shown in Fig. 7, which shows that the maximum output voltage of the bi-stable structure is always lower than that of the tri-stable structure at the same magnetic distance, regardless of the magnetic distance. The natural frequency of the bi-stable structure is around 7.8 Hz. As a result, when the frequency is greater than 7.8 Hz, the piezoelectric cantilever beam would cross the potential barrier, and the external excitation frequency starts to move away from the first-order intrinsic frequency of the piezoelectric cantilever beam, so the output voltage of the bi-stable structure starts to decrease. Similarly, the natural frequency of the tri-stable structure is around 10.2 Hz. As a result, when its frequency is greater than 10.2 Hz, the piezoelectric cantilever beam would cross the potential barrier, and the external excitation frequency is far away from the first-order intrinsic frequency of the piezoelectric cantilever beam, so the piezoelectric cantilever volume cannot do large vibration, causing the output voltage of the system starts to decrease.

Whether it is the bi-stable or the tri-stable, the output voltage of the system increases first and then decreases as the external excitation frequency increases. Compared to the tri-stable structure, the bi-stable one has a faster speed to reach the maximum output voltage of the system, which is determined by inherent frequencies of their different structures. Since the inherent frequency of the bi-stable structure is lower, it is suitable for collecting vibration energy at lower frequencies; while the inherent frequency of the tri-stable structure is higher, so it is suitable for collecting vibration energy at larger frequencies. However, in general, the maximum output voltage of

the tri-stable structure is higher than that of the bi-stable one.

3.2 The effect of external load resistance on system output power

In the field of electricity, the high voltage measured in the experiment does not mean the high output power of the system. Therefore, under the optimal output conditions of structure A and structure B, the effect of external load on the output power of the system is investigated. Also, through the analysis into measured data, the influence law of external load on the output power of the system of structure A and structure B can be obtained.

In the experiment, the magnetic spacing is 16 mm, the external excitation amplitude is set to 2.5 V, the external excitation frequency is 3–13.8 Hz with a step of 0.4 Hz, and the external load resistance is 800 k Ω , 600 k Ω and 500 k Ω . The results are shown in Fig. 8.

From Fig. 8, the system output power of structure A and structure B shows a trend of increasing and then decreasing, which is caused by the fact that the voltage of structure A and structure B first increases and then decreases. The output power of both structure A and structure B is maximum with the external load resistance of 600 k Ω , and the maximum output power is 106.07 μ W and 278.39 μ W respectively. As the external load resistance increases, the output power of the system starts to decrease, which shows that the output power of the system increases and then decreases with the increase of the external load resistance under the same external conditions. The overall output power of structure B is better than that of structure A. However, due to their different structures, structure A reaches the maximum output power earlier than structure B.

4 Summary and suggestions

In summary, this paper designs a tri-stable piezoelectric-electromagnetic composite energy harvester for capturing the lower frequencies of ambient vibration energy. The excellent structure of the harvester not only increases the stability of the system so that the harvester can better capture the ambient low frequency energy, but also improves the output voltage and energy conversion efficiency of the harvester. With an external excitation frequency of 10.2 Hz and a magnetic spacing of 16 mm, the TPEEH delivers a maximum output voltage of 12.0539 V, a generation efficiency of 0.223 V/mm³ and a maximum output power of 278.39 μ W at an external load resistance of 600 k Ω . Compared to the bistable composite energy harvester, the tri-stable structure produces the highest

maximum output voltage, power generation efficiency and output power, indicating that the tri-stable structure is more efficient in energy conversion than the bistable structure. The tri-stable piezo-electromagnetic composite energy harvester has potential applications in the large-scale exploitation of low-frequency vibration energy.

5 Fabrication of the TPEEH

In this design, the experimental fixture was modeled by Solidworks as a 3D solid and 3D printed with resin. The material of the piezoelectric beam is Cu with dimensions of 90mm × 20mm × 0.41mm, and the thickness of PVDF piezoelectric layer is 30 microns. The upper and lower layers of PVDF piezoelectric film are connected in series, and the piezoelectric film and the brass are pasted by conductive adhesive. The electromagnetic part consists of two coils and two springs. The springs used are soft ones, so that the connection between the magnet and the spring is easier to do reciprocal motion. The spring size is: 0.3 mm × 6 mm × 15 mm. The coil is a copper one whose size is: 14.4 mm × 20.5 mm × 13 mm. The size of the magnet used in the experiment is: 20 mm × 10 mm × 10 mm; the magnet of the electromagnetic part the and the spring are glued together with AB glue. All components would be left to stand for 24 h in a dry environment.

Data availability Authors state that data are available.

References

- Ali EK, Kyle J (2014) Efficiency enhancement of a cantilever-based vibration energy harvester. *Sensors* 14:188–211
- Arroyo E, Badel A, Formosa F et al (2012) Comparison of electromagnetic and piezoelectric vibration energy harvesters: model and experiments. *Sens Actuators A* 183:148–156
- Bolat FC, Basaran S, Sivrioglu S (2019) Piezoelectric and electromagnetic hybrid energy harvesting with low-frequency vibrations of an aerodynamic profile under the air effect. *Mech Syst Signal Process* 133:106246
- Iqbal M, Khan FU (2018) Hybrid vibration and wind energy harvesting using combined piezoelectric and electromagnetic conversion for bridge health monitoring applications[J]. *Energy Convers Manag* 172:611–618
- Javed U, Abdelkefi A (2019) Characteristics and comparative analysis of piezoelectric-electromagnetic energy harvesters from vortex-induced oscillations. *Nonlinear Dyn* 95:3309–3333
- Jiang SN, Li XF, Guo SH et al (2005) Performance of a piezoelectric bimorph for scavenging vibration energy. *Smart Mater Struct* 14(4):769–774
- Johnson TJ, Charnegie D, Clark WW et al (2006) Energy harvesting from mechanical vibrations using piezoelectric cantilever beams. In: *Proceedings of SPIE-The International Society for Optical Engineering*, University of Bristol, 61690D-61690D-12
- Khaligh, Onar OC (2009) CRC Press, Boca Raton
- Liu W, Han MD, Meng B et al (2014) Low frequency wide bandwidth MEMS energy harvester based on spiral-shaped PVDF cantilever. *Sci China Technol Sci* 57(6):1068–1072
- Mikio U, Kentaro N, Sadayuki U (1996) Analysis of the transformation of mechanical impact energy to electric energy using piezoelectric vibrator. *Jpn J Appl Phys* 35:3267–3273
- Roundy S, Wright PK (2004) A piezoelectric vibration based generator for wireless electronics. *Smart Mater Struct* 13(5):1131–1142
- Roundy S, Wright PK, Rabaey J (2003) A study of low level vibrations as a power source for wireless sensor nodes. *Comput Commun* 26(11):1131–1144
- Shindo Y, Narita E (2014) Dynamic bending/torsion and output power of S-shaped piezoelectric energy harvesters. *J Mech Mater Des* 10(3):305–311
- Sodano HA, Park G, Inman DJ (2004) Estimation of electric charge output for piezoelectric energy harvesting. *Strian* 40(2):49–58
- Song F, Xiong Y (2022) Design of a piezoelectric-electromagnetic hybrid vibration energy harvester operating under ultra-low frequency excitation. *Microsyst Technol* 28(8):1785–1795
- Toyabur RM, Salauddin M, Cho H et al (2018) A multimodal hybrid energy harvester based on piezoelectric-electromagnetic mechanisms for low-frequency ambient vibrations. *Energy Convers Manag* 168:454–466
- Wang ZW, Li TJ (2021) A semi-analytical model for energy harvesting of flexural wave propagation on thin plates by piezoelectric composite beam resonators. *Mech Syst Signal Process* 147:107137
- Wang X, Yang B, Liu J, Zhu Y, Yang C, He Q (2016) A flexible triboelectric-piezoelectric hybrid nanogenerator based on P(VDF-TrFE) nanofibers and PDMS/MWCNT for wearable devices. *Sci Rep* 6:36409
- Xia HK, Chen RW, Ren L (2015) Analysis of piezoelectric-electromagnetic hybrid vibration energy harvester under different electrical boundary conditions. *Sens Actuators A* 234:87–98
- Yang Y, Wang ZL (2015) Hybrid energy cells for simultaneously harvesting multi-types of energies. *Nano Energy* 14:245–256
- Yuzhong X, Fang S, Xinghuan L (2020) A piezoelectric cantilever-beam energy harvester (PCEH) with a rectangular hole in the metal substrate. *Microsyst Technol* 26(3):801–810

Publisher's Note Springer Nature remains neutral with regard to jurisdictional claims in published maps and institutional affiliations.

Springer Nature or its licensor (e.g. a society or other partner) holds exclusive rights to this article under a publishing agreement with the author(s) or other rightsholder(s); author self-archiving of the accepted manuscript version of this article is solely governed by the terms of such publishing agreement and applicable law.